# Factorization scale effects in QED corrections to $e^+e^-$- annihilation

U. E. Voznaya[1,2], A. B. Arbuzov[1,2]

[1]BLTP JINR

[2]Dubna State University

## Introduction

Current and future high-precision experiments require very accurate predictions that include calculation of higher-order contributions within perturbation theory. Computing the full $\mathcal{O}(\alpha^2)$ electroweak and even QED radiative corrections to realistic observables in high-energy physics remains a complex task. The QED structure function approach [1] circumvents this problem by taking into account higher-order contributions, amplified by the powers of the so-called large logarithm $L = \ln\frac{\mu_F^2}{\mu_R^2}$, where $\mu_F$ is the factorization scale and $\mu_R$ is the renormalization scale. In QED $\mu_R$ is usually chosen to be equal to the electron mass $m_e$. The choice of $\mu_F$ is somewhat arbitrary, but it should correspond to the characteristic energy scale of the process under consideration.

Terms of the order $\mathcal{O}(\alpha^n L^n)$ are usually called the leading logarithmic contributions (LL), and those of the order $\mathcal{O}(\alpha^n L^{n-1})$ are the next-to-leading logarithmic (NLL) ones, and so on.

Variation of the factorization scale leads to redistribution of contributions between terms with different powers of $L$ in horizontal lines of the following formal representation of radiative corrections

$$\begin{array}{llll} \alpha^0\ (\text{Born}) & & & \\ \alpha^1 L^1 & \alpha^1 L^0 & & \\ \alpha^2 L^2 & \alpha^2 L^1 & \alpha^2 L^0 & \\ \alpha^3 L^3 & \alpha^3 L^2 & \alpha^3 L^1 & \alpha^3 L^0 \\ \dots & & & \end{array}$$

For any given order in $\alpha$ the sum of all contributions with different powers of $L$ should not depend on the factorization scale.

Optimization of the scale choice should help to concentrate most of the corrections in terms with higher powers of the large logarithms, i.e., the LL and NLL ones, to reduce the contribution of the terms with lower powers of $L$ (and higher powers in $\alpha$) which are more difficult to calculate. This optimization will improve the convergence of perturbative calculations and reduce the theoretical uncertainty.

The process electron-positron annihilation into a virtual photon or $Z$ boson is considered [2]:

$$\begin{aligned} &e^-(p_1)+e^+(p_2)\to\gamma^*,Z\to\mu^-(q_1)+\mu^+(q_2)+(n\gamma,e^+e^-),\\ &s=(p_1+p_2)^2,\qquad s'=(q_1+q_2)^2=zs, \end{aligned} \tag{1}$$

where $(n\gamma,e^+e^-)$ means possible emitted photons and/or $e^+e^-$ pairs.

## Factorization scale choices in differential distribution

We analyze the applicability and effectiveness of various scale selection prescriptions for a specific QED process where analytical results are known for several orders in $\alpha$ and $L$. In parton distribution functions approach the cross section is represented in the Drell-Yan form

$$\begin{aligned} \frac{d\sigma_{\bar{e}e}^{\text{NNLL}}(s')}{ds'} &= \sum_{i,j=e,\bar{e},\gamma}\int_{\bar{z}_1}^1\int_{\bar{z}_2}^1 dz_1dz_2D_{i\bar{e}}^{\text{str}}\left(z_1,\frac{\mu_R^2}{\mu_F^2}\right)D_{j\bar{e}}^{\text{str}}\left(z_2,\frac{\mu_R^2}{\mu_F^2}\right)\\ &\times\left(\sigma_{ij}^{(0)}(sz_1z_2)+\bar{\sigma}_{ij}^{(1)}(sz_1z_2)+\bar{\sigma}_{ij}^{(2)}(sz_1z_2)\right)\delta(s'-sz_1z_2)+\mathcal{O}\left(\frac{m_e^2}{s}\right), \end{aligned} \tag{2}$$

where $D_{ie}^{\text{str}}(x,\mu_R^2/\mu_F^2)$ are the electron structure (parton density) functions [1, 3], $\bar{\sigma}_{ij}^{(1)}$ is one-loop and $\bar{\sigma}_{ij}^{(2)}$ is two-loop contribution to the annihilation sub-process cross section for massless partons computed within the $\overline{\text{MS}}$ scheme.

The master equation (2) for the cross section can be expanded as

$$\begin{aligned} \frac{d\sigma_{\bar{e}e}^{\text{NNLL}}(s')}{ds'} &= \frac{\sigma_{\bar{e}e}^{(0)}(s')}{s}\left\{\delta(1-z)+\sum_{\substack{k=1\\ l=k}}^{\infty}\left(\frac{\alpha}{2\pi}\right)^k c_{kl}(z)L^l\right.\\ &\left.+\sum_{\substack{k=1\\ l=k-1}}^{\infty}\left(\frac{\alpha}{2\pi}\right)^k c_{kl}(z)L^l+\sum_{\substack{k=1\\ l=k-2}}^{\infty}\left(\frac{\alpha}{2\pi}\right)^k c_{kl}(z)L^l+\mathcal{O}(\alpha^kL^{k-3})\right\}. \end{aligned} \tag{3}$$

Higher-order coefficients $c_{kl}(z)$ in the LL and NLL approximations up to $c_{65}$ were first calculated in [4], and some of them were independently recalculated and corrected in [2]. Explicit expression for $c_{20}$ can be found in [5].

A change of the factorization scale and the subsequent change of the large logarithm leads to redistribution of contributions in each order in $\alpha$. Let us now consider radiative corrections of the $\mathcal{O}(\alpha^2)$ order. Any change of the factorization scale must not change the full correction in the given order in $\alpha$ (and the complete result for the cross-section):

$$h_{22}+h_{21}+h_{20}=\hat{h}_{22}+\hat{h}_{21}+\hat{h}_{20}, \tag{4}$$

where we denote

$$h_{ij}\equiv\left(\frac{\alpha}{2\pi}\right)^i L^j c_{ij},\quad \hat{h}_{ij}\equiv\left(\frac{\alpha}{2\pi}\right)^i \hat{L}^j \hat{c}_{ij},\quad \hat{L}=\ln\frac{\hat{\mu}_F^2}{m_e^2}. \tag{5}$$

We consider changing the factorization scale as an addition to the large logarithm:

$$\hat{L}=L+\Delta L,\quad \Delta L=\ln\frac{\hat{\mu}_F^2}{\mu_F^2}, \tag{6}$$

and we get the matching equality:

$$\left(\frac{\alpha}{2\pi}\right)^2L^2c_{22}+\left(\frac{\alpha}{2\pi}\right)^2Lc_{21}+\left(\frac{\alpha}{2\pi}\right)^2c_{20}=\left(\frac{\alpha}{2\pi}\right)^2\hat{L}^2\hat{c}_{22}+\left(\frac{\alpha}{2\pi}\right)^2\hat{L}\hat{c}_{21}+\left(\frac{\alpha}{2\pi}\right)^2\hat{c}_{20}. \tag{7}$$

We get expressions for the new coefficients $\hat{c}_{ij}$:

$$\begin{aligned} \hat{c}_{22}&=c_{22},\\ \hat{c}_{21}&=c_{21}-2\Delta Lc_{22},\\ \hat{c}_{20}&=c_{20}-\Delta Lc_{21}+(\Delta L)^2c_{22}, \end{aligned} \tag{8}$$

We compare the initial factorization scale $\mu_F=\sqrt{s}$ with $\mu_F=\sqrt{sz}$ and $\mu_F=\sqrt{s/e}$. At $\sqrt{s}=240$ GeV we have the radiative return to the $Z$ resonance at $z\approx0.14$, where $sz=M_Z^2$. At $\sqrt{s}=160$ GeV the $Z$ resonance peak is at $z\approx0.32$. Let us look at the contributions to the differential cross section of the orders $\mathcal{O}(\alpha)$ and $\mathcal{O}(\alpha^2)$ at $\sqrt{s}=240$ GeV. The interval from $z=0$ to $z=1$ is divided into 20 bins and the integration was performed separately for each bin, starting from $z_{min}=0.05$. The histogram for the cross section with factorization scales equal to $\sqrt{s}$, $\sqrt{s/e}$, and $\sqrt{sz}$ (with the corresponding logarithms equal to $L$, $L-1$, and $L+\ln z$) and the difference between them in each bin are shown in the Figs. 1–1. Here $h_{i,tot}$ is a sum of all corrections of the given $i^{\text{th}}$ order in $\alpha$.

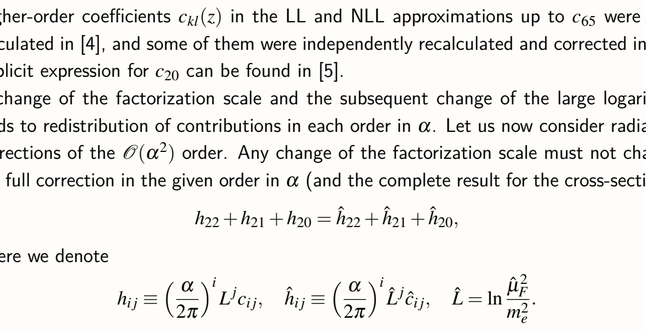


Figure 1: Corrections and differences for factorization scales $\sqrt{s}$, $\sqrt{s/e}$ (left), and $\sqrt{sz}$ (right), at $\mu_F^2$, $\mu_F^2/e$ and $\mu_F^2z$, $\sqrt{s}=240$, $\mathcal{O}(\alpha^1)$, in %

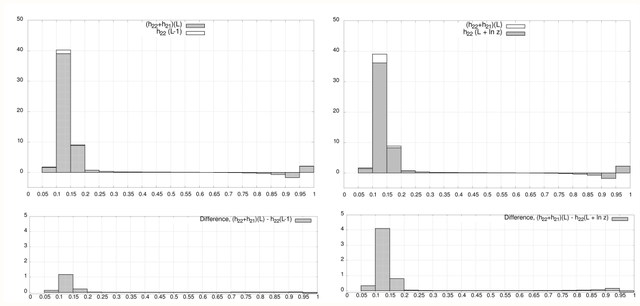


Figure 2: NLL corrections and differences for factorization scales $\sqrt{s}$, $\sqrt{s/e}$ (left), and $\sqrt{sz}$ (right) at $\mu_F^2$, $\mu_F^2/e$ and $\mu_F^2z$, $\sqrt{s}=240$, $\mathcal{O}(\alpha^2)$, in %

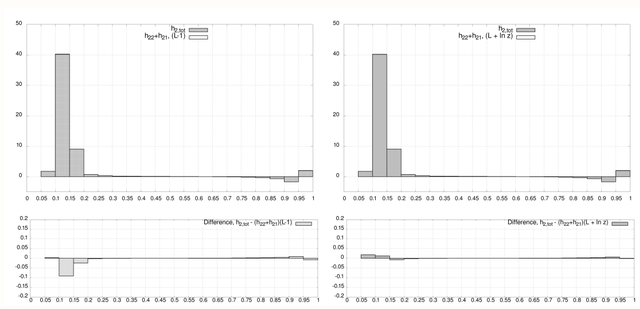


Figure 3: NNLL corrections and difference for factorization scales $\sqrt{s}$, $\sqrt{s/e}$ (left), and $\sqrt{sz}$ (right) at $\sqrt{s}=240$, $\mathcal{O}(\alpha^2)$ , in %

The preferred factorization scale appears to be $\sqrt{s/e}$, because with this scale in the order $\mathcal{O}(\alpha^1)$ the NLL contribution is almost completely (except the last bin) absorbed into LL one, see Fig. 1. A similar situation happens with the choice of the preferable factorization scale in the leading $\mathcal{O}(\alpha^2L^2)$ contribution (see Fig. 1).

But at the NLL level the sum of the $\mathcal{O}(\alpha^2L^2)$ and $\mathcal{O}(\alpha^2L^1)$ corrections (Fig. 1) for $\mu_F=\sqrt{sz}$ most NNLL contributions are absorbed into the NLL ones. Note that this happened for the integrated (over bins) distribution and for the particular choice of the c.m.s. energy.

## Factorization scale choices in the total cross section

To obtain the total cross-section we integrate the differential one from some $z_{min}$, defined by experimental conditions, to 1. By integrating the corrected cross section from $z_{min}=0.1$ to 1 at $\sqrt{s}=240$ GeV, we include the contribution due to the radiative return to the $Z$ resonance into the integration domain, and that yields unusually large corrections. Thus, at $e^+e^-$ colliders with energies above the $Z$ peak, one can expect quite a lot of events due to radiative return to the peak, and the theoretical uncertainties in the description of such events will suffer from large, yet unknown, higher-order contributions. Figs. 4 and 5 show the LL and NLL corrections as a function of the factorization scale choice with $z_{min}=0.1$. They are compared to the results with the factorization scale $\mu_F=\sqrt{sz}$, the corresponding lines are marked $h_{ij}(L+\ln z)$. The center-of-mass (c.m.s.) energies are 240 GeV and 3 TeV, which correspond to the optimal energy of associated production of Higgs and $Z$ bosons and to the maximal energy of the CLIC collider project, respectively. The factorization scale varies from 10 GeV to the maximal c.m.s. energy.

Table 1: Corrections of the order $\mathcal{O}(\alpha^2)$ in % to the total cross section for $\sqrt{s}=240$ GeV and 3 TeV at different $z_{min}$

| | | 240 GeV | | | 3 TeV | | |
|---|---|---|---|---|---|---|---|
| | | $z_{min}=0.1$ | $z_{min}=0.5$ | $z_{min}=0.9$ | $z_{min}=0.1$ | $z_{min}=0.5$ | $z_{min}=0.9$ |
| $h_{22}+h_{21}+h_{20}$ | | 50.7861 | −0.8667 | 0.3082 | 1.1518 | −1.1524 | 0.5320 |
| $h_{22}+h_{21}$ | $\sqrt{s}$ | 49.9954 | −0.8812 | 0.3063 | 1.1092 | −1.1656 | 0.5302 |
| | $\sqrt{sz}$ | 49.8924 | −0.8838 | 0.3052 | 1.1044 | −1.1683 | 0.5291 |
| | $\sqrt{s/e}$ | 50.0130 | −0.8841 | 0.3086 | 1.1071 | −1.1682 | 0.5325 |
| $h_{22}$ | $\sqrt{s}$ | 52.4634 | −0.9954 | 0.3793 | 1.0772 | −1.2869 | 0.6229 |
| | $\sqrt{sz}$ | 44.9544 | −0.9508 | 0.4077 | 0.8922 | −1.2342 | 0.6565 |
| | $\sqrt{s/e}$ | 48.5231 | −0.9206 | 0.3508 | 1.0092 | −1.2057 | 0.5836 |

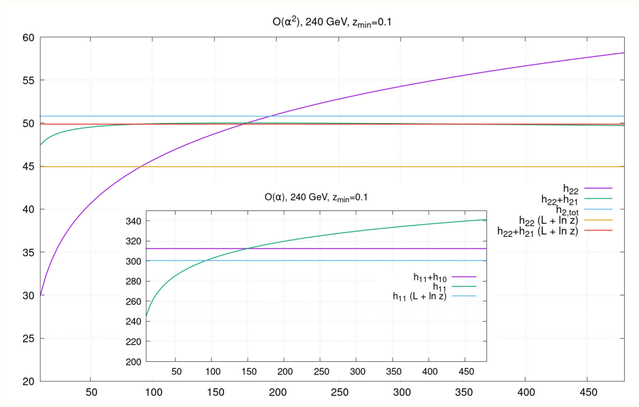


Figure 4: Corrections vs. factorization scale for $\sqrt{s}=240$ GeV, $z_{min}=0.1$

The complete correction of the particular order in $\alpha$ does not depend on the factorization scale. Figs. 4 and 5 show the $\mathcal{O}(\alpha^1)$ and $\mathcal{O}(\alpha^2)$ corrections with different scaling for better readability.

One can see that the leading logarithmic contributions $h_{11}$ and $h_{22}$ strongly depend on $\mu_F$, while in the next-to-leading approximation the dependence becomes rather weak. The conventional choice of the factorization scale $\mu_F=\sqrt{sz}$ is certainly not optimal in the LL approximation, but occasionally it works reasonably well in the NLL case.

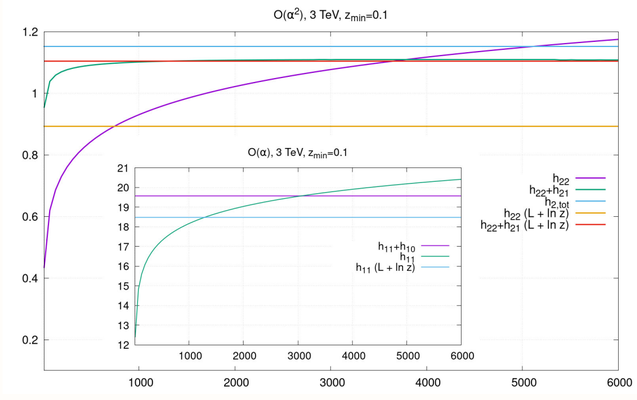


Figure 5: Corrections vs. factorization scale for $\sqrt{s}=3$ TeV, $z_{min}=0.1$

## Estimation of the uncertainties

Estimation of the uncertainties by varying the factorization scale by factors $1/2$ and 2 is a common procedure in QCD. We choose the central value of the factorization scale $\mu_F=\sqrt{s}$ and compute $h_{22}$, $h_{22}+h_{21}$, and $h_{33}$ at factorization scales $2\mu_F$ and $\mu_F/2$. The results are shown in Table 2. Here $\Delta^{LL}$ are $h_{21}$ and $h_{32}$, and $\Delta^{NLL}$ is $h_{20}$ at the central value of the factorization scale. So, $\Delta^{LL}$ and $\Delta^{NLL}$ are the true values of the shifts due to "unknown contributions" if one works in the LL and NLL approximations, respectively. Quantities $\delta^{LL}$ and $\delta^{NLL}$ show the average shifts of the LL and NLL contributions due to the factorization scale variation. So, $\delta_{LL,NLL}$ are estimated shifts of the same "unknown contributions". The true and estimated shifts are defined as follows:

$$\begin{aligned} \Delta_2^{\text{LL}}&=|h_{21}|,\\ \Delta_2^{\text{NLL}}&=|h_{20}|,\\ \delta_2^{\text{LL}}&=\frac{|h_{22}-h_{22}(1/2)|+|h_{22}-h_{22}(2)|}{2},\\ \delta_2^{\text{NLL}}&=\frac{|h_{22}+h_{21}-(h_{22}+h_{21})(1/2)|}{2}\\ &+\frac{|h_{22}+h_{21}-(h_{22}+h_{21})(2)|}{2},\\ \Delta_3^{\text{LL}}&=|h_{32}|,\\ \delta_3^{\text{LL}}&=\frac{|h_{33}-h_{33}(1/2)|+|h_{33}-h_{33}(2)|}{2}, \end{aligned} \tag{9}$$

where $h_{ij}(2)$ and $h_{ij}(1/2)$ are $h_{ij}$ at factorization scales $2\mu_F$ and $\mu_F/2$ correspondingly, and $h_{ij}$ without argument are $h_{ij}$ at initial factorization scale.

The numerical results for the shifts are given in Table 2. It is seen that at the energies above the $Z$ peak (for $\sqrt{s}=240$ GeV or 3 TeV) for $z_{min}=0.1$ the estimated shifts $\delta_2^{\text{NLL}}$ and $\delta_3^{\text{LL}}$ seriously underestimate the corresponding true values. For $\sqrt{s}=240$ GeV at $z_{min}=0.1$ the radiative return to the resonance is taken into account, while for $\sqrt{s}=3$ TeV it contributes only for $z_{min}<0.001$.

Table 2: Calculated and estimated uncertainties in %

| | $\mathcal{O}(\alpha^2)$ | | | | $\mathcal{O}(\alpha^3)$ | |
|---|---|---|---|---|---|---|
| | LL | | NLL | | LL | |
| | $\Delta_2^{\text{LL}}$ | $\delta_2^{\text{LL}}$ | $\Delta_2^{NLL}$ | $\delta_2^{\text{NLL}}$ | $\Delta_3^{\text{LL}}$ | $\delta_3^{\text{LL}}$ |
| $\sqrt{s}=M_z$, $z_{min}=0.1$ | 0.436 | 0.524 | 0.0064 | 0.0250 | 0.0250 | 0.0499 |
| $\sqrt{s}=M_z$, $z_{min}=0.5$ | 0.436 | 0.5246 | 0.0063 | 0.0250 | 0.0249 | 0.0499 |
| $\sqrt{s}=M_z$, $z_{min}=0.9$ | 0.440 | 0.529 | 0.0063 | 0.0252 | 0.0249 | 0.0497 |
| $\sqrt{s}=240$ GeV, $z_{min}=0.1$ | 2.468 | 5.569 | 0.5178 | 0.1479 | 0.5833 | 0.1015 |
| $\sqrt{s}=240$ GeV, $z_{min}=0.5$ | 0.1142 | 0.1057 | 0.0088 | 0.0061 | 0.0014 | 0.0002 |
| $\sqrt{s}=240$ GeV, $z_{min}=0.9$ | 0.073 | 0.0403 | 0.0019 | 0.0039 | 0.0216 | 0.0294 |
| $\sqrt{s}=3$ TeV, $z_{min}=0.1$ | 0.0320 | 0.0958 | 0.0240 | 0.0021 | 0.0307 | 0.0126 |
| $\sqrt{s}=3$ TeV, $z_{min}=0.5$ | 0.1213 | 0.1145 | 0.0082 | 0.0054 | 0.0034 | 0.0018 |
| $\sqrt{s}=3$ TeV, $z_{min}=0.9$ | 0.0926 | 0.0554 | 0.0020 | 0.0041 | 0.0298 | 0.0402 |

## Summary and Conclusions

- In the considered process of electron-positron annihilation high values of the factorization scale of the order of the initial center-of-mass energy $\mu_F\approx\sqrt{s}$ or $\mu_F\approx\sqrt{s/e}$ are preferable. This choice is in accord with the prescription provided by the fastest apparent convergence method.
- We verified the validity of the standard scale uncertainty estimation procedure by varying it by a factor of 2. We found that the procedure provides reasonable numerical estimates for most setups, except for the crucial case of radiative return to a resonance or just to lower energy of the hard subprocess. In the latter case, the standard method greatly underestimates the uncertainty.
- Our results are relevant for constructing an advanced treatment of higher-order QED corrections for electron-positron annihilation processes studied at current and future colliders.
- Some of the presented results may also be relevant for QCD, in particular, for description of Drell-Yan-like processes at LHC.

## References

[1] E. A. Kuraev and Victor S. Fadin. Sov. J. Nucl. Phys., 41:466–472, 1985.

[2] A. B. Arbuzov and U. E. Voznaya, Phys. Rev. D 109, 113002 (2024), arXiv:2405.03443 [hep-ph].

[3] A.B. Arbuzov, U.E. Voznaya, arXiv: 2212.01124 [hep-ph]

[4] J. Ablinger, J. Blümlein, A. De Freitas, and K. Schönwald, Nucl. Phys. B 955, 115045 (2020), arXiv:2004.04287 [hep-ph]

[5] J. Blümlein, A. De Freitas, C.G. Raab, K. Schönwald, Phys.Lett.B 791 (2019), 206-209, arXiv: 1901.08018 [hep-ph]